Molecular Structure of Gaseous Titanium Tris(tetrahydroborate), $Ti(BH_4)_3$: Experimental Determination by Electron Diffraction and Molecular Orbital Analysis of some $Ti(BH_4)_3$ Derivatives†

C. John Dain,[a] Anthony J. Downs,*[,a] Michael J. Goode,[a] David G. Evans,*[,b] Karen T. Nicholls,[b] David W. H. Rankin*[,c] and Heather E. Robertson[c]

[a] *Inorganic Chemistry Laboratory, University of Oxford, Oxford OX1 3QR, UK*

[b] *Department of Chemistry, University of Exeter, Exeter EX4 4QD, UK*

[c] *Department of Chemistry, University of Edinburgh, Edinburgh EH9 3JJ, UK*

The structure of gaseous titanium tris(tetrahydroborate) has been determined by analysis of the electron diffraction patterns due to the molecules $Ti(BH_4)_3$ and $Ti(BD_4)_3$. The molecule has thus been shown to possess three tridentate BH_4 groups generating a structure with C_{3h} symmetry overall, implying nine-fold co-ordination of the titanium atom and a *planar* TiB_3 skeleton. With the assumption of local C_{3v} symmetry for each $Ti(BD_4)$ fragment, salient structural parameters (r_a) are as follows: r(Ti···B) 217.5(0.4), r(Ti–D_b) 198.4(0.5), r(B–D_b) 127.6(0.5) and r(B–D_t) 116.6(1.3) pm; and *within* each $Ti(BD_4)$ fragment D_b–Ti–D_b 60.1(0.7) and D_b–B–D_b 102.4(0.6)°. Such a structure is consistent with the IR and UV photoelectron spectra of the molecule in the gaseous or matrix-isolated states, but aggregation occurs in the condensed phases (*e.g.* in solution in a non-polar solvent or in the solid state). The structural properties of the $Ti(BH_4)_3$ molecule are compared with those of related tetrahydroborate derivatives, and the factors influencing these properties are assessed in terms of elementary symmetry and perturbation-theory arguments, supported by extended Hückel molecular orbital calculations.

Transition-metal tetrahydroborates command attention on several counts.[1,2] From a practical standpoint, they are potentially important as precursors to solid metal borides,[3] to metal hydrides,[4] as well as alkyls;[5] they may also function as olefin polymerization catalysts.[6] From a structural standpoint, they are intriguing for the versatility displayed by the tetrahydroborate group in the mode of its ligation to the metal centre which may entail triple,[1] double[1] or single[4e,7] hydrogen bridges. Although the UV photoelectron spectra of some of the simpler volatile tetrahydroborates have been investigated,[8] theoretical discussions have been confined mainly to qualitative molecular orbital (MO) arguments drawing, for example, on the isolobality principle.[9,10] This is all the more surprising because the structure, bonding and conformational variations displayed by derivatives of the BH_4^- anion may hold vital clues to the activation of the isoelectronic CH_4 molecule.

The connection between BH_4^- and CH_4 finds its most obvious expression in the remarkable structure **I** revealed recently for the crystalline bis(trimethylphosphine) adduct of titanium tris(tetrahydroborate), $Ti(BH_4)_3(PMe_3)_2$.[11] Not only is the bonding mode of two of the BH_4^- groups reminiscent of the 'agostic' interaction between ligand methyl groups and certain metal centres,[12] exemplified by the Ti···H–C interaction **II** featured by the crystalline titanium(IV) complex $MeTiCl_3(Me_2PCH_2CH_2PMe_2)$,[13] it also resembles closely one of the proposed transition states for the activation of alkanes.[14]

Yet about the volatile, thermally fragile parent titanium tetrahydroborate, $Ti(BH_4)_3$, there is a dearth of well authenticated information, problems of decomposition or contamination by halide or neutral donor molecules tending to cloud the picture.[15] In 1982 some of us reported the preliminary results of an electron diffraction study involving the gaseous $Ti(BH_4)_3$ molecule and concluded, on the basis of measurements made at a single, relatively long camera distance, that it contains triply bridged tetrahydroborate groups generating nine-fold co-ordination of the titanium atom.[16] Here we present the results of a more complete study, incorporating electron diffraction measurements on the molecule $Ti(BD_4)_3$ at short, as well as long, camera distances, and IR measurements on both $Ti(BH_4)_3$ and $Ti(BD_4)_3$ in the vapour and matrix-isolated states. Analysis of the findings confirms the earlier structural conclusions while pointing now, not to a pyramidal, but to a planar, TiB_3 skeleton. The structure thus conforms to the expectations of a theoretical analysis supported by extended Hückel MO calculations,[17,18] and we draw on this analysis to elucidate the factors which determine (*i*) the geometry of the TiB_3 skeleton and (*ii*) the co-ordination mode of the BH_4^- ligands. In common with other mononuclear titanium(III) species, such as $(\eta^5\text{-}C_5H_5)_2TiCl$,[19a] and (cyclo-$C_6H_{11})_7Si_7O_{12})Ti$,[19b] but not $(\eta^5\text{-}C_5Me_5)_2TiCl$,[19c] titanium tris(tetrahydroborate) is subject to aggregation in the condensed phases.

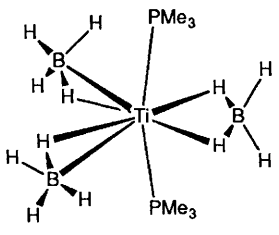

I

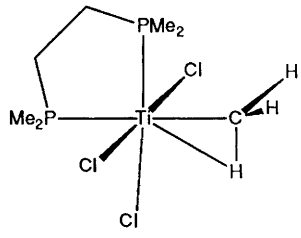

II

† *Non-SI units employed:* Torr ≈ 133 Pa, eV ≈ 1.6 × 10^{-19} J.

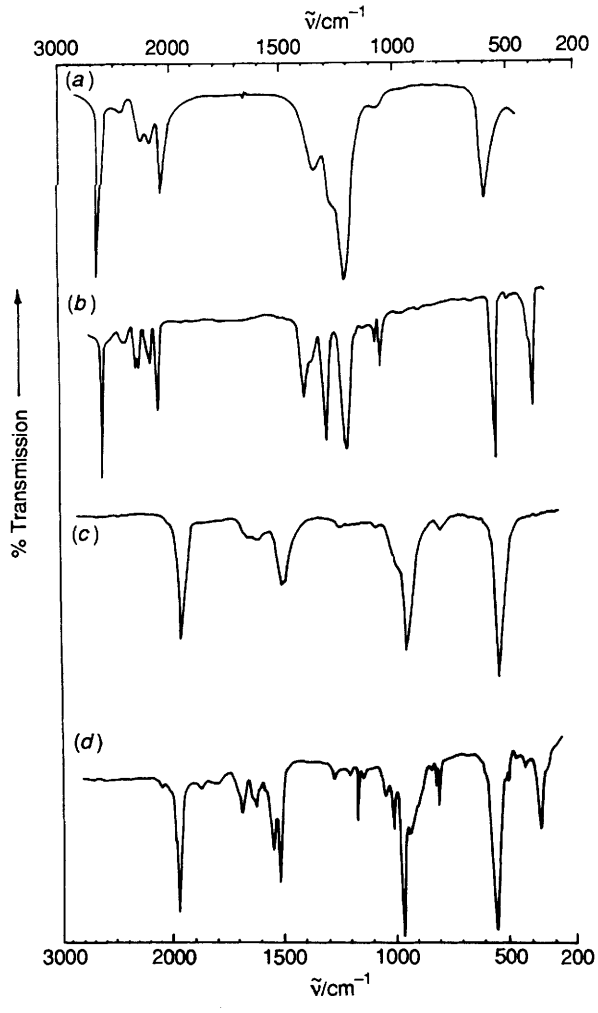

Fig. 1 Infrared spectra of $Ti(BH_4)_3$ and $Ti(BD_4)_3$. (*a*) $Ti(BH_4)_3$ vapour, pressure *ca.* 1 Torr, 290 K; (*b*) $Ti(BH_4)_3$ isolated in an Ar matrix at *ca.* 15 K [Ar:$Ti(BH_4)_3$ = *ca.* 300:1]; (*c*) $Ti(BD_4)_3$ vapour, pressure *ca.* 1 Torr, 290 K; and (*d*) $Ti(BD_4)_3$ isolated in an Ar matrix at *ca.* 15 K [Ar:$Ti(BD_4)_3$ = *ca.* 300:1]. The vapour samples were contained in a Pyrex glass cell with a pathlength of 10 cm fitted with CsI windows

When dissolved in a hydrocarbon solvent, for example, it exists predominantly in the form of a dimer, $[Ti(BH_4)_3]_2$.[20]

Results and Discussion

Synthesis and Characterisation of $Ti(BH_4)_3$.—The reaction of titanium tetrachloride with an excess of lithium tetrahydroborate, which proceeds ideally in accordance with equation (1)

$$2TiX_4 + 8LiBH_4 \longrightarrow 2Ti(BH_4)_3 + 8LiX + B_2H_6 + H_2 \quad (1)$$

(with X = Cl), is the normal synthetic route giving access to titanium tris(tetrahydroborate).[11,15] A major problem is posed, however, by the close similarity in volatility of the compounds $Ti(BH_4)_3$ and $ClTi(BH_4)_2$ which precludes their complete separation by fractional sublimation *in vacuo*.[15] Under the conditions needed to secure a product free from co-ordinated solvent molecules, there is therefore a serious risk of contamination by chloride impurity, a factor undoubtedly contributing to confusion and discrepancies, not only between different sets of published results,[15] but also between these results and the findings of the present research.[20]

For this reason we have turned to titanium tetrabromide as the precursor to titanium tris(tetrahydroborate) [equation (1) (with X = Br)]. Although bromotitanium derivatives of the type $Br_nTi(BH_4)_{3-n}$ have not been characterised, it is reasonable to expect any such compound to be significantly less volatile than $ClTi(BH_4)_2$ or $Ti(BH_4)_3$. This has two obvious advantages: (*i*) there is less chance that any bromotitanium tetrahydroborate intermediate will vaporise before the reaction can proceed to completion; and (*ii*) there is likely also to be a marked improvement in the efficiency of vacuum sublimation as a means of separating the tris(tetrahydroborate) from any potential halogenotitanium contaminants. The change of strategy has proved highly successful. Titanium tetrabromide vapour is drawn *slowly* through a bed of freshly recrystallised lithium tetrahydroborate at room temperature. The volatile products are withdrawn under continuous pumping and separated by fractional condensation. Pure titanium tris(tetrahydroborate) can be isolated, after repeated fractionation, in yields of about 80% based on the amount of titanium tetrabromide taken and consumed in accordance with equation (1).

The properties of the compound in solution (*e.g.* in a non-polar solvent such as hexane) and in the solid state point to pronounced aggregation of the $Ti(BH_4)_3$ molecules.[20] For example, vapour-pressure measurements on isopentane solutions imply that the predominant solute species is not the monomer but the dimer $[Ti(BH_4)_3]_2$. This conclusion is supported by the ^1H and ^{11}B NMR spectra of [$^2H_8$]toluene solutions which bear witness to the presence of a *diamagnetic* species containing two distinct types of tetrahydroborate groups in the proportions 2:1. The most likely explanation involves the formation of a relatively loosely bound dimer incorporating bridging and terminal tetrahydroborate groups, as in **III**. The solid titanium compound exists in several different

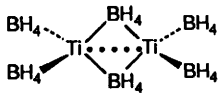

III

phases the optical and IR properties of which suggest significant variations in the mode of co-ordination of the BH_4^- ligands. Hence it is clear that the properties of the condensed phases cannot be trusted for any positive characterisation of the $Ti(BH_4)_3$ monomer.

Accordingly, we now focus on the vapour species and examine their IR and UV photoelectron spectra for information bearing on the structural model most likely to provide a working basis for interpreting the measured electron diffraction pattern.*

Infrared Spectra of Gaseous and Matrix-isolated $Ti(BH_4)_3$ *and* $Ti(BD_4)_3$.—Infrared spectra have been measured for the isotopically normal and perdeuteriated versions of titanium tris(tetrahydroborate), with reference to both the vapour at ambient temperatures and to the vapour species trapped in an excess of argon at *ca.* 15 K. The relevant results are illustrated in Fig. 1 and itemised in Table 1. The results are subject to several complications and limitations. First, the sample of $Ti(BD_4)_3$ was contaminated with small amounts of incompletely deuteriated isotopomers such as $Ti(BD_4)_2(BD_3H)$. Matrix isolation of the tetrahydroborate, while sharpening its IR bands and facilitating the identification of some features, gave rise to two potential sources of confusion. One was the splitting of several of the bands, presumably as a result of the trapping of $Ti(BH_4)_3$ molecules in different matrix sites, although one cannot rule out the trapping of different conformers. In addition, the spectrum of a matrix sample typically included a

* The reactivity and low thermal stability of the compound thwarted attempts to measure a meaningful mass spectrum of the vapour.

Table 1 Infrared bands (cm^{-1}) exhibited by gaseous and matrix-isolated $Ti(BH_4)_3$ and $Ti(BD_4)_3$ in the region 200–4000 cm^{-1}

$Ti(BH_4)_3$		$Ti(BD_4)_3$		
a	*b*	*a*	*b*	Assignment[c]
			2000–2650w	^1H impurity
	2595(sh)		1958(sh)	
2585s	2585s	1938s	1944s	$\nu(B–H_t)$
2400w (br)	2370w (br)			2 × *ca.* 1200
			1845w (br)	1493 + 352
			1710–1800w	^1H impurity
	2270m		1680(sh)	
2230mw	2230m	1650w	1658w	
2155mw	2160m	1600w	1610mw	$\nu(B–H_b)$
	2130m		1596w	
			1578w	
			1559w	^1H impurity
			1524m	
2030m	2035ms	1495ms	1493ms	$\nu(B–H_b)$
			1130–1260w	^1H impurity
	1365ms			
1345m	1330m	1030(sh)	1030m	
1265(sh)	1276s	1000(sh)	994m	$\delta(H_b–B–H_t)$
1210s (br)	1195s	945s	952vs	
	1150vw[d]		992m[d]	
			870(sh)[d]	$[Ti(BH_4)_3]_x$ aggregate
			823vs[d]	
1075w (br)	1077w		806w	
	1052w	807w	792m	$\delta(H_b–B–H_t)$
	608(sh)			
595ms	598s	540s	544vs	$\nu(Ti–B)$
	536w[d]		486m[d]	$[Ti(BH_4)_3]_x$ aggregate
			453vw	^1H impurity
			415w[d]	$[Ti(BH_4)_3]_x$ aggregate
450w	454ms	325w	352ms	$Ti(H_b)_3B$ deformation
			325(sh)[d]	$[Ti(BH_4)_3]_x$ aggregate

s = Strong, m = medium, w = weak, v = very, sh = shoulder and br = broad.
[a] Vapour at *ca.* 290 K. [b] In argon matrix at *ca.* 15 K. [c] H_t = terminal H atom, H_b = bridging H atom. [d] Band grows when the matrix is annealed.

number of weak features which were observed to grow at the expense of the principal features (*i*) when the matrix was annealed or (*ii*) when the matrix concentration of the tetrahydroborate was increased. This behaviour, allied to the prominence of bands with the same or similar energies in the spectra of the compound in the condensed phases,[20] leaves little doubt that the bands in question originate, not from monomeric $Ti(BH_4)_3$, but from an aggregate such as $[Ti(BH_4)_3]_2$. Close scrutiny has revealed, for example, that a band at 536 cm^{-1}, which was identified originally with the symmetric Ti–B stretching fundamental of $Ti(BH_4)_3$,[16] shows all the signs of belonging to such an aggregate. There are also limitations imposed partly by the low pressure of the vapour ($\leqslant$1 Torr) and partly by the restricted wavenumber range of the measurements (200–4000 cm^{-1}). Hence it follows that the spectra are necessarily incomplete.

In spite of the complications and deficiencies, the spectra lend themselves satisfactorily to analysis in terms of the group vibrations of the discrete molecules $Ti(BH_4)_3$ and $Ti(BD_4)_3$, with the assignments specified in Table 1. Such an analysis has been based on three main criteria: (*i*) analogies with related molecules containing a co-ordinated tetrahydroborate group;[1,21] (*ii*) the selection rules expected to govern the activity in IR absorption of the vibrational fundamentals associated with different structural models of the $Ti(BH_4)_3$ molecule; and (*iii*) the effect of deuteriation at the BH_4^- group on the energy of a given spectroscopic feature. Wavenumbers quoted in parentheses refer to the species $Ti(BD_4)_3$ in the following discussion.

The first salient point is the observation of a single intense absorption at 2585 (1938) cm^{-1}; taken in conjunction with the absence of any doublet near 2500 cm^{-1}, this is characteristic of tridentate tetrahydroborate groups.[1,21] Other features diagnostic of tridentate binding of the tetrahydroborate group are to be found in the appearance (*a*) of a doublet of medium-to-weak intensity near 2200 cm^{-1} and (*b*) of an intense band near 1200 cm^{-1}.[1,21] The case for tridentate binding is reinforced, moreover, by the resemblance which $Ti(BH_4)_3$ bears, in both the wavenumbers and intensity pattern of its IR spectrum, not only to the tetrahydroborates $Zr(BH_4)_4$[22] and $Hf(BH_4)_4$,[23] for which definitive structures have been determined,[24,25] but also to the actinide derivatives $M(BH_4)_4$ (M = U,[26] Np[27,28] or Pu[27]), which are believed to form molecules isostructural with $Zr(BH_4)_4$ and $Hf(BH_4)_4$ in the gas phase. That there is no sign of the features characteristic of bidentate binding, as exhibited, for example, by the molecule $Al(BH_4)_3$,[29] gives us good grounds for believing that the tetrahydroborate groups are bound to the metal in $Ti(BH_4)_3$ *exclusively via* triple hydrogen bridges. The crystal structures of several tetrahydroborates, *e.g.* $Ti(BH_4)_3(PMe_3)_2$[11] and $U(BH_4)_4$,[30] serve as a warning that, even within a single molecule, such uniformity is by no means assured.

In a variety of possible structures for the $Ti(BH_4)_3$ molecule, depending on the form of the heavy-atom skeleton and the precise disposition of the bridging hydrogen atoms, we identify three likely options. The first of these (**IV**) involves a planar TiB_3 skeleton; the BH_4^- groups are then arranged so that one bridging hydrogen atom of each group is coplanar with this skeleton to complete a model with C_{3h} symmetry. The second (**V**) involves a pyramidal TiB_3 skeleton with the BH_4^- groups arranged to comply with C_{3v} symmetry. The third (**VI**) acknowledges the possibility of a less symmetrical variant of **IV** and **V** in which the BH_4^- groups are no longer correlated to

Table 2 Correlation of the fundamentals of a single $Ti(\mu\text{-}H)_3BH$ moiety with C_{3v} symmetry with those of a $Ti(BH_4)_3$ molecule having C_{3h}, C_{3v} or C_3 symmetry overall and comparison of the predicted with the experimental results

			$Ti(BH_4)_3$ molecule[d]						
			Model **IV**, C_{3h} symmetry		Model **V**, C_{3v} symmetry		Model **VI**, C_3 symmetry		
Approximate description of mode[a]	Expected wavenumber range[b]/cm^{-1}	$Ti(\mu\text{-}H)_3BH$ moiety with C_{3v} symmetry Irred. rep.[c]	Irred. rep.[c]	No. of IR-active modes	Irred. rep.[c]	No. of IR-active modes	Irred. rep.[c]	No. of IR-active modes	No. of IR bands observed
$\nu(B\text{–}H_t)$	2450–2600	a_1	a′ + e′	1	a_1 + e	2	a + e	2	1
$\nu(B\text{–}H_b)$	2000–2300	a_1	a′ + e′	1	a_1 + e	2	a + e	2	3
		e	a′ + a″ + e′ + e″	2	$a_1 + a_2$ + 2e	3	2a + 2e	4	
$\delta(H_b\text{–}B\text{–}H_t)$ + $\nu(Ti\text{–}H_b)$	1000–1400	a_1	a′ + e′	1	a_1 + e	2	a + e	2	
		e	a′ + a″ + e′ + e″	2	$a_1 + a_2$ + 2e	3	2a + 2e	4	4–5
		e	a′ + a″ + e′ + e″	2	$a_1 + a_2$ + 2e	3	2a + 2e	4	
$Ti(\mu\text{-}H)_3B$ deformation + $\nu(Ti\text{–}H_b)$	400–650	e	a′ + a″ + e′ + e″	2	$a_1 + a_2$ + 2e	3	2a + 2e	4	1–2
$\nu(Ti\text{–}B)$	550–650	a_1	a′ + e′	1	a_1 + e	2	a + e	2	1
TiB_3 skeletal deformation	<250	—	a′ + e′	1	a_1 + e	2	a + e	2	—[e]
$Ti(\mu\text{-}H)_3B$ torsion	<250	—	a″ + e″	1	a_2 + e	1	a + e	2	—[e]

[a] Descriptions of modes are based on those suggested by a normal coordinate analysis of the molecule $Zr(BH_4)_4$. See ref. 22. t = terminal, b = bridging. [b] See, for example, refs. 1, 21 and 22. [c] Irreducible representation. [d] See text for details. [e] Features probably fall outside the range of the current measurements.

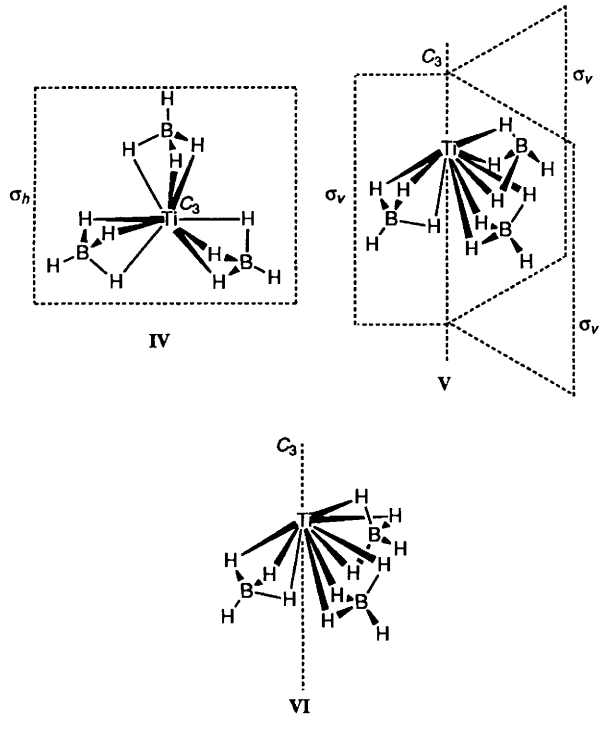

optimise the symmetry and the molecule achieves a symmetry no higher than C_3. Table 2 lists the numbers and irreducible representations of the vibrational fundamentals appropriate to each of the models **IV**–**VI**; the resulting predictions are presented in the form of a region-by-region survey which draws on the group-vibration terminology favoured by Smith *et al.*[22] on the strength of their normal coordinate analysis of the related molecule $Zr(BH_4)_4$.

Three sets of assignments are relatively straightforward. These involve the stretching vibrations of the terminal and bridging B–H bonds, $\nu(B\text{–}H_t)$ and $\nu(B\text{–}H_b)$, respectively, and the Ti–BH_4 stretching vibration, $\nu(Ti\text{–}B)$ (see Table 1). In every case the number of bands is entirely consistent with the vibrational properties expected of the model **IV** with C_{3h} symmetry, while falling short of the number of IR-active fundamentals predicted for the models **V** and **VI**. Absorptions in the range 1000–1400 (750–1050) cm^{-1} are almost certainly due to fundamentals in which H–B–H bending is the predominant motion.[22] Although there is some uncertainty about the exact number, there are at least four, and possibly five, such bands, a conclusion also consistent with the requirements of model **IV** (see Table 2). This leaves outstanding just one feature located near 450 (325) cm^{-1}, which shows signs of being a doublet in the matrix spectrum; this we are inclined to assign to one or two skeletal fundamentals involving deformation of the $Ti(\mu\text{-}H)_3B$ bridges.[22]

UV Photoelectron Spectrum of Gaseous $Ti(BH_4)_3$.—The helium I and helium II excited photoelectron spectrum of gaseous titanium tris(tetrahydroborate) contains just three bands at low binding energies, the associated ionisation energies being 8.97, 11.2 and 12.7 eV. Lowest in energy is the feature corresponding to the '3d' ionisation, whereas the two broad and partially overlapping features at higher energy are attributable to ionisation (*i*) from orbitals localised mainly on the BH_4^- ligands (11.2 eV) and (*ii*) from orbitals localised in the hydrogen bridges and therefore representing metal–ligand bonding orbitals (12.7 eV). The finding that the cross-section for ionisation near 12.7 eV is appreciably greater than that for ionisation near 11.2 eV means that $Ti(BH_4)_3$ shows the intensity pattern characteristic of molecules like $Zr(BH_4)_4$, $Hf(BH_4)_4$ and $U(BH_4)_4$ which contain tridentate BH_4^- groups.[8] Quite a different pattern characterises molecules like $Al(BH_4)_3$ containing bidentate BH_4^- groups.[8,31]

Electron Diffraction Measurements and Structure Refinement.—The radial distribution curve derived from the electron-scattering pattern of gaseous $Ti(BD_4)_3$ is illustrated in Fig. 2. It contains four main peaks which can easily be identified as follows. The prominent peak near 120 pm must correspond to scattering from the B–D_b and B–D_t atom pairs. The most intense peak near 215 pm reflects a blend of contributions from Ti–B and Ti–D_b atom pairs. At longer distances there are two weaker features: that near 330 pm can be correlated with scattering from the non-bonded Ti···D_t atom pairs, that near 375 pm with scattering from the non-bonded B···B atom pairs. Still weaker and less well defined features of the curve also take account of scattering from non-bonded B···D and D···D atom pairs. On the other hand, the absence of significant scattering from atom pairs separated by more than about 400 pm argues against the presence in the

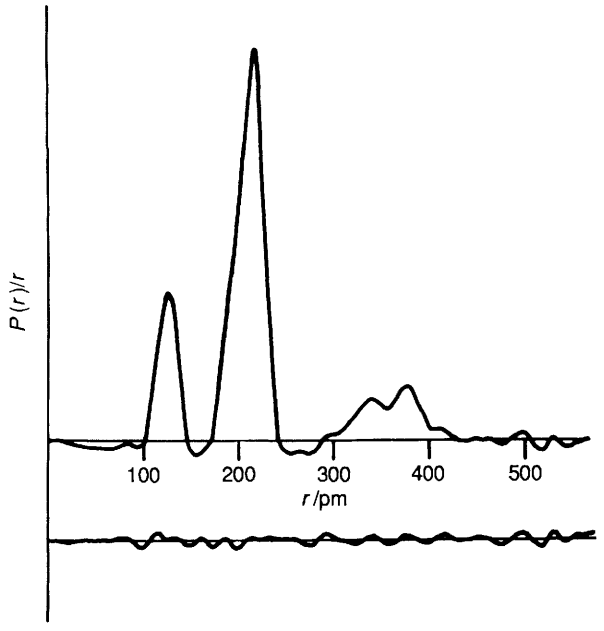

Fig. 2 Observed and difference radial distribution curves, $P(r)/r$ *vs.* r, for $Ti(BD_4)_3$. Before Fourier transformation, the data were multiplied by $s.\exp[(-0.000\,015\,s^2)/(Z_{Ti} - f_{Ti})(Z_B - f_B)]$

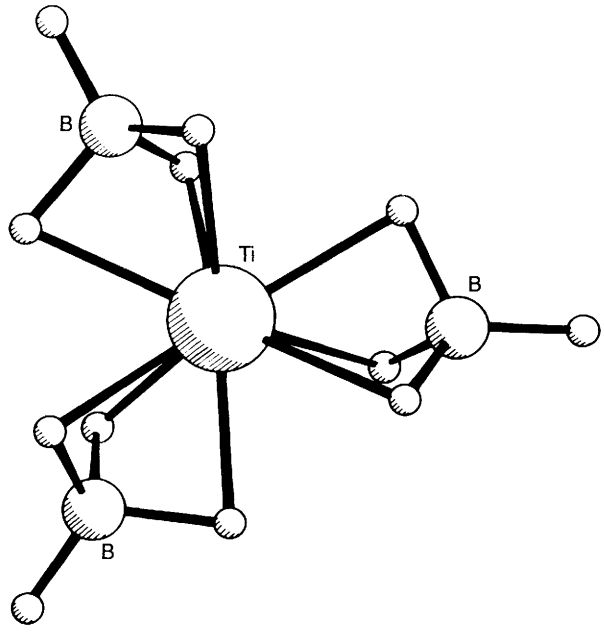

Fig. 3 Perspective view of the molecule $Ti(BD_4)_3$ (along the C_3 axis) in the optimum refinement of the electron diffraction data

vapour of more than trace amounts of any oligomeric species, *e.g.* $[Ti(BD_4)_3]_2$, a conclusion consistent with our reading of the IR spectrum.

As a basis for calculating the electron-scattering intensities of $Ti(BD_4)_3$, we adopted initially a model along the lines of **IV**, but including some provision for exploring the precise geometry of the TiB_3 skeleton and the orientation of the $Ti(\mu\text{-}D)_3B$ units. In all, this model required six independent geometrical variables to be specified. With reference to Fig. 3, the variables comprised (*i*) the Ti–D_b distance; (*ii*) a mean B–D distance; (*iii*) the difference $\Delta(B\text{–}D) = r(B\text{–}D_b) - r(B\text{–}D_t)$ between the bridging and terminal B–D distances; (*iv*) the Ti–B distance; (*v*) a 'dip' angle, θ, specifying the angle subtended by each Ti–B vector with respect to a plane normal to the C_3 axis; and (*vi*) a 'twist' angle, τ, which enabled all three $Ti(\mu\text{-}D)_3B$ groups to be rotated in a *concerted* fashion about the C_3 axis each of them was assumed to have, with $\tau = 0$ corresponding to the conformation where one D atom of each group is located in the plane taken initially to define the TiB_3 skeleton (*i.e.* $\theta = 0$). The initial model with $\theta = 0$ and $\tau = 0$ corresponds, then, to **IV** with C_{3h} symmetry.

All of the distances responded satisfactorily to refinement, as did the amplitudes of vibration associated with the Ti–B, Ti–D_b, Ti ••• D_t, B–D and B ••• B distances. Other vibrational amplitudes, which made only a small contribution to the overall molecular scattering, were assigned values based on the precedents set by related molecules, *e.g.* $Zr(BH_4)_4$,[24] $Al(BH_4)_3$[32] and B_2H_6.[33] More problematic were the two angles θ and τ, neither of which refined particularly well. The earlier analysis of $Ti(BH_4)_3$ seemed to imply a value of θ near 12°,[16] although it was appreciated at the time that this could be an artifact of 'shrinkage effects'; moreover, the use of only a single data set for $Ti(BH_4)_3$* meant that the measurements were of a sensitivity lower than usual, and subject to poorer resolution of closely similar distances, notably Ti–B and Ti–H_b. The optimum fit to the electron scattering for $Ti(BD_4)_3$ was obtained with $\theta = 4.2°$, but in the later stages of refinement θ varied from about zero to 7°, and the e.s.d. associated with the optimum value was $\pm 3.7°$. The twist angle, τ, varied in the later stages of refinement within the range $8 \pm 9°$. The extended Hückel calculations, to be discussed in the next section, suggest that the potential wells defined by both of these co-ordinates are shallow, with the result that large amplitudes govern the motions distorting the molecule from its rest configuration. Even with deuteriation, the estimated amplitudes of vibration associated with the hydrogen bridges are still quite large, with a Ti–D_b amplitude considerably larger than either the Ti–B or B–D amplitude (see Table 3). This feature reflects the unsymmetrical nature of the Ti–D_b–B bridges, with the D_b atom being bound more tightly to the boron than to the titanium atom. Indeed, given the small amplitude of vibration of the Ti–B atom pair, it is arguable that the best simple description of the bonding is given by the model **VII**.

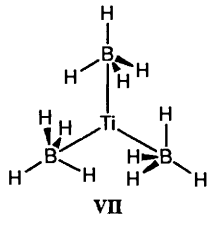

VII

The 'side-on' ligation favoured by two of the BH_4^- groups in the phosphine complex $Ti(BH_4)_3(PMe_3)_2$[11] led us to investigate whether something similar might also occur in the parent molecule $Ti(BH_4)_3$. The possibility of distortion of the triple hydrogen bridges was admitted to the model used in the preceding calculations *via* a single parameter φ allowing each $Ti(\mu\text{-}D)_3B$ unit to be deformed so that the plane described by the three D atoms was no longer normal to the Ti–B axis, while one D atom was confined to the plane of the TiB_3 skeleton. Irrespective of whether positive or negative values were tried for φ, any departure from $\varphi = 0$ resulted in an overall increase in the R factor which could be achieved in the subsequent refinement calculations. Hence there is no reason to believe that the molecule $Ti(BH_4)_3$ favours the unsymmetrical mode of co-ordination found in $Ti(BH_4)_3(PMe_3)_2$.[11] Calculations were also carried out with a model having two of the BH_4^- groups

* It proved impossible to measure any useful scattering for $Ti(BH_4)_3$ at short nozzle-to-plate distances. Whether the success in recording such scattering for $Ti(BD_4)_3$ was a fortuitous result of slightly higher ambient temperatures, the use of a better-than-average filament in the electron gun or the preparation of a sample purer than that used in the earlier measurements is not clear. The use of a heated inlet system was precluded, however, by the limited thermal stability of the compound.

Table 3 Molecular parameters deduced from the electron diffraction pattern of $Ti(BD_4)_3$

(*a*) Independent geometrical parameters: distances (pm), angles (°), r_a structures[a]

Parameter	Magnitude	Magnitude of corresponding parameter in $Ti(BH_4)_3$[b]
p_1 $r(Ti–D_b)$	198.4 (0.5)	206.7 (1.7)
p_2 $r(B–D)_{mean}$	124.8 (0.4)	119.9 (0.4)
p_3 $r(Ti–B)$	217.5 (0.4)	221.8 (1.5)
p_4 $\Delta(B–D) = r(B–D_b) – r(B–D_t)$	11.0 (1.5)	12.3 (2.5)
p_5 Skeletal 'dip' angle, θ[c]	4.2 (3.7)	12.0 (1.6)
p_6 $B(D_b)_3$ 'twist' angle, τ[c]	7.8 (8.0)	—

(*b*) Interatomic distances (r_a/pm), bond angles (°) and amplitudes of vibration (u/pm)[a]

	$Ti(BD_4)_3$		$Ti(BH_4)_3$[b]	
Parameter	Distance or angle	Amplitude	Distance or angle	Amplitude
$r(Ti–D_b)$	198.4 (0.5)	10.9 (0.7)	206.7 (1.7)	8.5 (2.0)
$r(B–D_b)$	127.6 (0.5)	4.7 (1.1)	123.0 (0.8)	4.5 (1.9)
$r(B–D_t)$	116.6 (1.3)	4.7[d]	110.7 (2.1)	4.5[d]
$r(Ti–B)$	217.5 (0.4)	5.6 (0.5)	221.8 (1.5)	9.8 (1.2)
$r(B \cdots B)$	375.8 (1.5)	11.0 (1.6)	375.8 (1.5)	9.1 (1.4)
$r(Ti \cdots D_t)$	334.1 (1.5)	13.8 (2.2)	332.5 (1.5)	14.8 (2.8)
$r(D_b \cdots D_b)$[e]	211.0 (2.7)	30.0[f]		
$r(D_b \cdots D_b)$[g]	198.8 (0.7)	10.0[f]		
$r(D_b \cdots D_t)$[g]	207.0 (1.1)	10.0[f]		
B–Ti–B	119.5 (0.6)	—	115.8 (0.7)	—

[a] Figures in parentheses are the estimated standard deviations of the last digits. [b] Calculations relate to measurements made at a single camera distance (see ref. 16); main parameters only listed. [c] For definition see text. [d] Constrained to be equal to $u(B–D_b)$ [or $u(B–H_b)$]. [e] Shortest $D_b \cdots D_b$ distance for D_b attached to *different* B atoms. [f] Fixed. [g] For D atoms attached to the *same* B atom.

Table 4 Portion of the least-squares correlation matrix listing off-diagonal elements with absolute values >50%; k_2 is a scale factor

$u(Ti–D_b)$	$u(B–D_b)$	$u(Ti–B)$	k_2	
−72				p_3
	−77			p_4
		62		$u(Ti–D_b)$
			53	$u(Ti–B)$

triply hydrogen-bridged and the third doubly hydrogen-bridged, but these too gave an inferior account of the electron-scattering pattern.

There is insufficient independent information to admit the possibility of making quantitative corrections for shrinkage, but we have no reason to suppose that such corrections would alter significantly the results of the analysis. The success of that analysis may be gauged numerically by the final R_G value of 0.069 (R_D = 0.061) and graphically by the difference between the experimental and calculated radial distribution curves (see Fig. 2); Fig. 4 compares the experimental and calculated molecular scattering. Although there is some correlation implicating certain vibrational amplitudes, particularly those associated with Ti–B and Ti–D_b atom pairs (see Table 4), the main features of the structure are well determined.

The structure of $Ti(BD_4)_3$ resembles most obviously those of $Zr(BH_4)_4$[24] and $Hf(BH_4)_4$,[25] at least with regard to the geometry of the individual $M(\mu\text{-}H)_3BH$ moieties (M = Ti, Zr or Hf), while also inviting comparisons with those of other titanium tetrahydroborates, *e.g.* $Ti(BH_4)_3(PMe_3)_2$[11] and $(\eta^5\text{-}C_5H_5)_2TiBH_4$,[34] the corresponding aluminium compound, $Al(BH_4)_3$,[32] and a variety of other metal tetrahydroborates. Collation of the dimensions of some of these species (see Table 5) is revealing for the light it sheds on the stereochemical properties of the co-ordinated BH_4^- group. The results highlight the short Ti–B distance (217.5 pm) in $Ti(BD_4)_3$, associated presumably with increased metal–boron bonding, as well as the elongation of the Ti–D_b bonds, both features characteristic of the tridentate mode of co-ordination. With bidentate BH_4^- groups, the Ti–B distance varies appreciably but is typically about 235 pm. The increase of about 17.5 pm compares with the value of 24 pm predicted by Edelstein[39] on the basis of his estimates of the effective ionic radii of bidentate and tridentate BH_4^- anions. The variation of the distances and the discrepancy reflect the difficulties of trying to extend the notion of an ionic radius to any system with a substantial degree of covalent bonding.

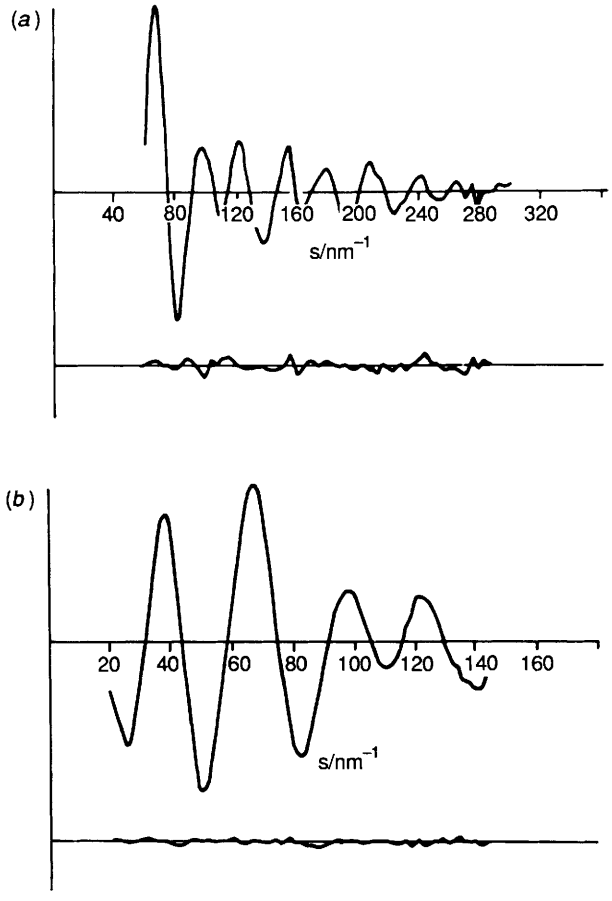

Fig. 4 Experimental and final difference molecular-scattering intensity curves for $Ti(BD_4)_3$; nozzle-to-plate distances (*a*) 128.4 and (*b*) 285.2 mm

There are few, if any, well authenticated systems involving titanium(III) in a three-co-ordinate or pseudo-three-co-ordinate environment with which $Ti(BH_4)_3$ is obviously comparable. About the shapes of the gaseous trihalide molecules there seems to be little unambiguous information.[40] The nearest analogy seems to be with the amido derivative $Ti[N(SiMe_3)_2]_3$ which is believed to have a planar TiN_3 skeleton, although the precise details are sparse.[41] The planarity of the TiB_3 skeleton in $Ti(BH_4)_3$ comes therefore as no particular surprise, although there are some theoretical grounds hinting at a pyramidal structure;[42] the essential point is that the issue of its planarity seems no longer to be in doubt.

Theoretical Considerations: Extended Hückel MO Calculations.—The tetrahedral BH_4^- anion is characterised by filledB–H bonding MOs (of a_1 and t_2 symmetry in the T_d point

Table 5 A comparison of the dimensions of $Ti(BD_4)_3$ with those of some related metal tetrahydroborates (distances in pm)

Molecule	Phase/method/ co-ordination mode[a]	r(M–B)	r(M–H_b)	r(B–H_b)	r(B–H_t)	Ref.
$Ti(BD_4)_3$	Vapour/ED/tridentate	217.5(4)	198.4(5)	127.6(5)	116.6(13)	This work
$Zr(BH_4)_4$	Vapour/ED/tridentate	230.8(3)	221.1(14)	127.2(18)	118(4)	24
$(\eta^5\text{-}C_5H_5)_2TiBH_4$	Vapour/ED/bidentate	231(4)	189(5)	—[b]	—[b]	34*b*
$Al(BH_4)_3$	Vapour/ED/bidentate	214.3(3)	180.1(6)	128.3(12)	119.6(12)	32
$Hf(BH_4)_4$	Crystal/ND/tridentate	225(3)	206(3)	119(2)	131(2)	25
$U(BH_4)_4$	Crystal/ND/tridentate	252(1)	234(2)	123(4)	124(4)	26
$Np(BH_4)_4$	Crystal/XD/tridentate	246(3)	220(50)	115(20)	100(30)	27, 28
$Ti(BH_4)_3(PMe_3)_2$	Crystal/XD/bidentate	240(1)	190(6)	103(7)	100(8)	11
	+ unsymmetrical tridentate	227(1)	173(7), 225(7), 262(7)	95(6)	96(6)	
$Ti(BH_4)_2(dmpe)_2$[c]	Crystal/XD/bidentate	253.4(3)	204(2), 209(2)	115(2)	112(3)	7*d*
$[(\eta^5\text{-}C_5H_5)TiCl(BH_4)]_2$	Crystal/XD/bidentate	217(1)	194(7)	107–118	104	35
$(\eta^5\text{-}C_5H_5)_2TiBH_4$	Crystal/XD/bidentate	237(1)	175(8)	123(8)	140(10)	34*a*
$V(BH_4)_2(dmpe)_2$[c]	Crystal/XD/unidentate	283.3(4)	188(3)	112(3)	103(5)	7*d*
$CuBH_4(PMePh_2)_3$	Crystal/XD/unidentate	251.8(3)	169.7(5)	117.0(5)	123(5)	7*a*
$CuBH_4(PPh_3)_2$	Crystal/XD/bidentate	218.5(6)	182(3)	107(3)	109(5)	36
$V(BH_4)_3(PMe_3)_2$	Crystal/XD/bidentate	236.5(6)	184(3)	119(3), 109(3)	104(5), 102(4)	37
$[V(BH_4)_2(PMe_3)_2]_2O$	Crystal/XD/bidentate	238.3(6)	197(3)	115(4)	109(4)	37
$Sc(BH_4)_3(thf)_2$[d]	Crystal/XD/tridentate	222.9(5), 233.0(5)	209(5) (mean)	108(5) (mean)	108(5) (mean)	38
	+ bidentate	255.1(5)				

[a] ED, electron diffraction; ND, neutron diffraction; XD, X-ray diffraction. [b] Dimensions not reported. [c] dmpe = $Me_2PCH_2CH_2PMe_2$. [d] thf = tetrahydrofuran.

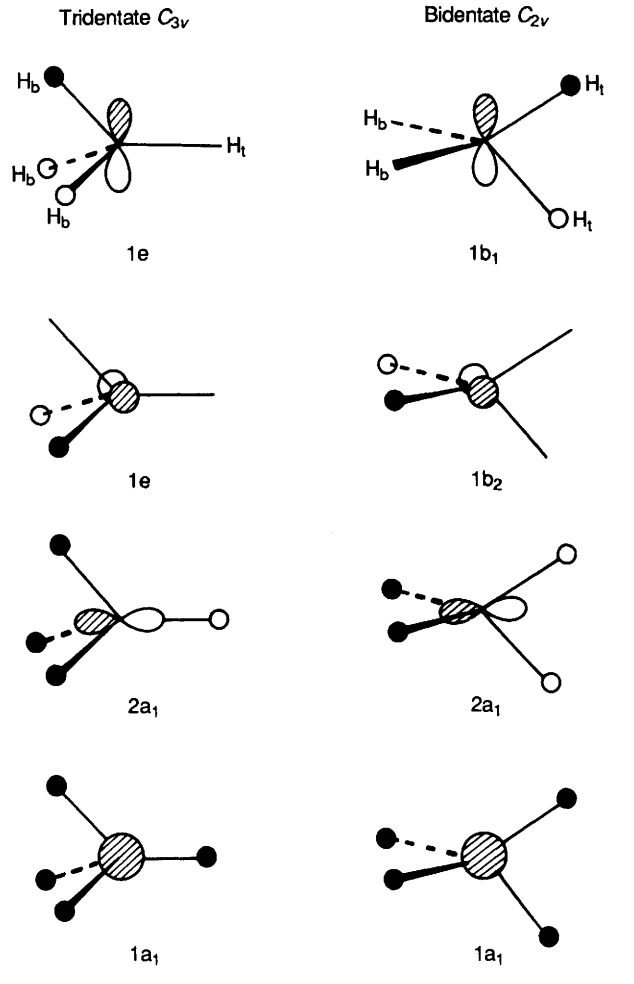

Fig. 5 Occupied frontier orbitals of the BH_4^- ligand. In the tridentate co-ordination mode the $2a_1$ and 1e orbitals are effective in donating electron density to the metal, whereas in the bidentate co-ordination mode only two orbitals ($2a_1$ and $1b_2$) are effective in this way

group) and four vacant B–H antibonding MOs (also of a_1 and t_2 symmetry).[43] When co-ordinated to a metal M, the local symmetry about the boron atom is reduced, to C_{3v} in the case of the tridentate and C_{2v} in the case of the bidentate mode of binding. Co-ordination thus lifts the degeneracy of the t_2 sets, to $a_1 + e$ in C_{3v} and $a_1 + b_1 + b_2$ in C_{2v} symmetry. In the first case, the four occupied BH_4^- orbitals transform as $2a_1 + e$, of which the a_1 orbitals may be described as σ-type and the e orbitals as π-type with respect to M–BH_4 bonding, as illustrated in Fig. 5. The lower $1a_1$ orbital interacts only poorly with the metal and remains localised mainly on the ligand, so that the BH_4^- ligand effectively furnishes three filled donor orbitals (σ + 2π) for binding to the metal. To a first approximation, therefore, BH_4^- resembles Cl^-. In the bidentate mode of co-ordination the lower $1a_1$ orbital again overlaps only very slightly with the metal, as does one of the M–BH_4 π orbitals ($1b_1$) which is localised on the boron and terminal hydrogen atoms. It follows that the ligand now has two effective frontier orbitals (one σ- and one π-type with respect to M–BH_4 bonding) and acts, to a first approximation, as a four-electron donor like phosphide, PR_2^-.

We consider first the tridentate mode of co-ordination. For a model planar $TiCl_3$ species, with D_{3h} symmetry, the ligand orbitals generate three M–L σ-type bonding ($a_1' + 1e'_\sigma$) and six π-type ($a_2' + a_2'' + 2e'_\pi + e''$) symmetry-adapted linear combinations. An early transition metal like titanium has 3d orbitals that are relatively diffuse and so make the major contribution to metal–ligand bonding. The ($d_{x^2-y^2}$, d_{xy}) and (d_{xz}, d_{yz}) sets of metal orbitals find a match with the ligand $2e'_\pi$ and e″ sets, respectively. The ligand a_1', $1e'_\sigma$ and a_2'' orbitals are, by contrast, stabilised more weakly by interaction with the metal 4s and 4p orbitals, whereas the ligand a_2' combination is constrained strictly to be non-bonding under D_{3h} symmetry. The metal d_{z^2} orbital is also approximately non-bonding since the overlap with the ligand a_1' combination in the *xy* plane is very poor. The position is shown schematically in Fig. 6. When the Cl^- ligands are replaced by tridentate BH_4^- groups, however, the symmetry of the resulting assembly is reduced from D_{3h}. One possible arrangement of the bridging hydrogen atoms has C_{3h} (**IV**), whereas another has C_{3v} symmetry (**V** but with a planar MB_3 skeleton). The MO schemes for these two

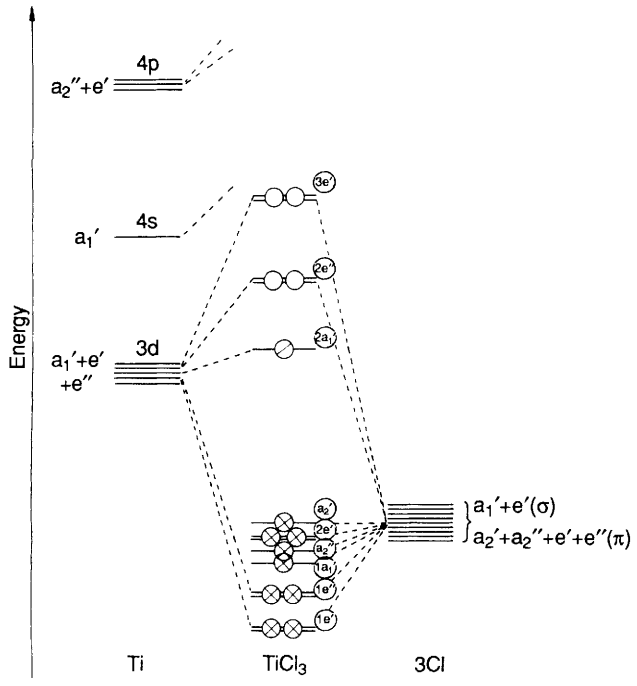

Fig. 6 Molecular orbital diagram corresponding to the formation of the planar $TiCl_3$ molecule. Four of the ligand symmetry-adapted linear combinations are strongly stabilised by overlap with metal d orbitals (giving 1e′ and 1e″ MOs), and four more weakly by overlap with metal s and p orbitals. The ligand a_2' orbital is non-bonding on symmetry grounds, and the metal d_{z^2} orbital is also approximately non-bonding

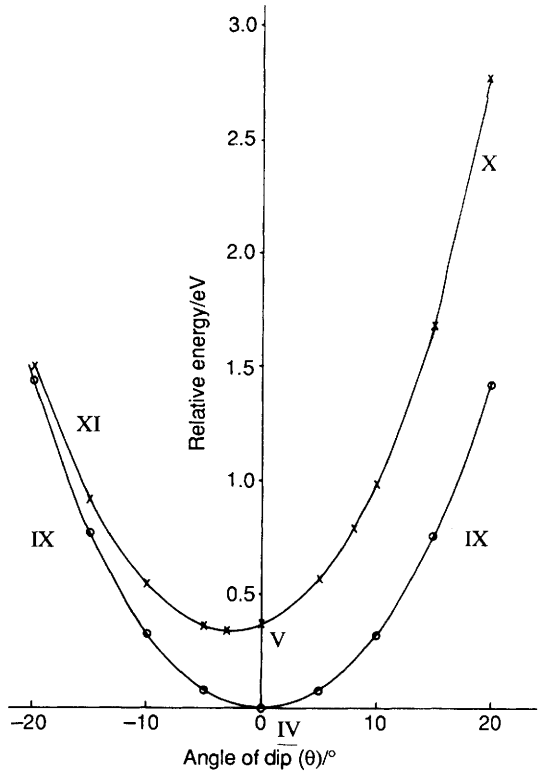

Fig. 7 Total energies of the $Ti(BH_4)_3$ molecule calculated for different angles of 'dip', θ, relative to the configuration with C_{3h} symmetry (**IV**) and showing the effects of distorting the planar TiB_3 skeleton to a pyramidal form

arrangements broadly resemble that of Fig. 6, but with one major difference. For the transformation $D_{3h} \longrightarrow C_{3h}$ both the representations a_2' and a_1' correlate with a′. Hence the descendant of the a_2' ligand combination and d_{z^2} are able to overlap, enhancing electron donation to the metal. Since the bonding component of this interaction is fully occupied, whilst the antibonding component is only semi-occupied, there is therefore a net stabilisation. The highest-occupied molecular orbital (HOMO) and semi-occupied molecular orbital (SOMO) of **IV** are represented as **VIIIa** and **VIIIb**,

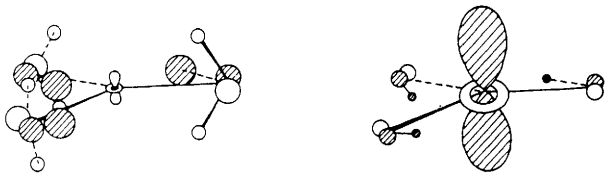

VIIIa **VIIIb**

respectively. With the alternative C_{3v} geometry (**V**), however, this mixing is not allowed since the descent of symmetry $D_{3h} \longrightarrow C_{3v}$ carries the following implications: $a_1' \longrightarrow a_1$ and $a_2' \longrightarrow a_2$; therefore the ligand combination deriving from the a_2' set remains non-bonding. Extended Hückel calculations suggest indeed that the C_{3h} conformer **IV** lies 0.37 eV (36 kJ mol^{-1}) lower in energy than the C_{3v} one **V** and that the charge on the titanium atom is lower in the former case (+0.67 *vs.* +0.75). For small angles of twist away from C_{3h} symmetry, the potential energy surface is very flat [the energy required for a 10° distortion being only 0.08 eV (8 kJ mol^{-1})].

We consider next the distortion of the C_{3h} and C_{3v} planar structures to give pyramidal TiB_3 skeletons. In the former case, a structure with C_3 geometry is generated (**IX**); in the latter case, two alternative structures **X** and **XI**, both retaining C_{3v} symmetry, are feasible. The energy changes which accompany the distortion **IV** ⟶ **IX** and **X** ⟵ **V** ⟶ **XI** are illustrated in Fig. 7. The transformation $C_{3h} \longrightarrow C_3$ means the loss of the molecular mirror plane in **IX**, leading to a loss of the distinction between a′ and a″ and between e′ and e″ orbitals. Mixing between orbitals within the a and e manifolds under C_3 symmetry leads to a series of four-electron destabilising interactions which oppose the process of pyramidalisation. On the other hand, the minimum of the potential energy curve associated with the distortion is quite shallow, with the energy required for a 10° departure from planarity being 0.33 eV (32 kJ mol^{-1}).

The C_{3h} geometry lies at an overall energy minimum, and a pyramidal C_3 structure such as **IX** is lower in energy than either of the corresponding C_{3v} structures **X** and **XI** for any value of

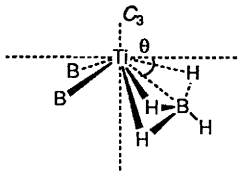

IX (C_3)

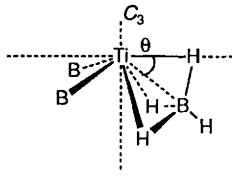

X (C_{3v})

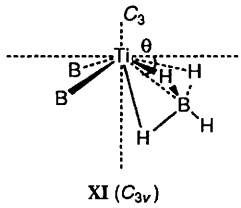

XI (C_{3v})

the 'dip' angle, θ, specifying the departure from planarity of the TiB_3 skeleton (see Fig. 7). This reflects the condition that the ligand-based a_2 orbital in the D_{3v} conformers is always unavailable for bonding to the metal.

For the ground-state C_{3h} structure the computed Mulliken overlap populations are as follows: Ti–B 0.25; Ti–H_b 0.19; B–H_b

0.59; B–H_t 0.83. Although it is not meaningful directly to compare Mulliken overlap populations between pairs of different atoms,[44] the calculations do show that there is significant direct Ti–B overlap and that the B–H_b overlap population is a substantial fraction of the B–H_t overlap population. The populations are also consistent with the large amplitude of vibration inferred for the Ti–D_b and the comparatively small amplitude of vibration inferred for the Ti–B vectors on the evidence of the electron-scattering pattern.

In the case of bidentate BH_4^- ligands, one can envisage two symmetrical species, **XII** and **XIII**, of which only **XII**

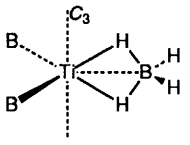

XII (D_{3h})

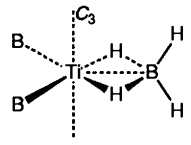

XIII (D_{3h})

[corresponding to the structure of $Al(BH_4)_3$][32] is feasible on steric grounds. As noted already, one of the ligand π-type orbitals overlaps but poorly with the metal orbitals, being localised mainly on the boron and terminal hydrogen atoms; by contrast, the other π-type orbital, which is localised on the boron and bridging hydrogen atoms, acts as a very effective electron donor to the metal. The second orbital generates an e″ combination which interacts with the metal (d_{xz}, d_{yz})(e″) set under the D_{3h} symmetry of structure **XII**. The exact energy difference between **IV** and **XII** depends on the Ti–B distance in the hypothetical molecule **XII**. The switch from tridentate to bidentate co-ordination of BH_4^- is typically attended by an increase in the metal–boron distance.[1,39] With a Ti–B distance equal to 237 pm, the value determined for the corresponding distance in $(\eta^5\text{-}C_5H_5)_2TiBH_4$,[34a] **XII** is calculated to lie at an energy 0.43 eV (41.5 kJ mol^{-1}) above that of **IV** and to have a higher positive charge on the titanium atom (+1.08 *vs.* +0.67 in **IV**). Although **IV** thus emerges as the ground-state structure, there is clearly scope for facile fluxional exchange of the hydrogen atoms *via* a bidentate intermediate or transition state. The energy barrier to interchange of hydrogen atoms is calculated to be lower than 0.43 eV if the bidentate BH_4^- ligand establishes a Ti–B contact shorter than 237 pm or if only one or two of the ligands exchange the tridentate for the bidentate mode of co-ordination.

It is noteworthy that bidentate co-ordination of the BH_4^- ligand should be adopted by $(\eta^5\text{-}C_5H_5)_2TiBH_4$[34] yet be unfavourable in the case of $Ti(BH_4)_3$. The apparent anomaly may be readily understood by reference to the frontier orbitals of the angular $(\eta^5\text{-}C_5H_5)_2Ti$ fragment. As shown by Lauher and Hoffmann,[45] these comprise two orbitals of σ symmetry and one of π symmetry with respect to the putative Ti–B axis. The π-type orbital lies in the mirror plane between the two rings, as shown in **XIV**, and is ideally disposed to interact with one filled

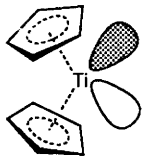

XIV

π-donor orbital of the BH_4^- ligand. At the same time there is no vacant metal orbital to stabilise the orthogonal π-donor orbital of the ligand and therefore the bidentate co-ordination mode, where this orbital remains localised on the ligands avoiding a four-electron destabilising interaction, is now made energetically favourable.

We have also examined a third possible co-ordination mode

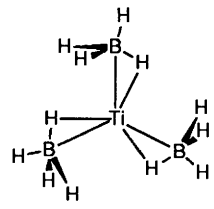

XV

in which $Ti(BH_4)_3$ emulates the phosphine complex $Ti(BH_4)_3(PMe_3)_2$[11] by forming highly unsymmetrical triple hydrogen bridges having one short and two long Ti–H_b contacts (*cf.* **I**). A distortion of this nature, whilst maintaining C_{3h} molecular symmetry overall to give **XV**, has two main effects. First, the bonding overlap with the out-of-plane metal orbitals d_{z^2}, d_{xz} and d_{yz} is reduced as the out-of-plane hydrogen atoms are bent away from the metal. Secondly, the distinction between in-plane ligand orbitals as possessing either σ or π symmetry with respect to the Ti–B vector is lost on distortion, a feature which leads to four-electron destabilising interactions between filled metal–ligand bonding MOs (1e′ and 2e′ in Fig. 6). Such a distortion is therefore predicted to be energetically unfavourable. For example, if the in-plane Ti–H_b distance is reduced to 170 pm whilst the other two are increased to 239 pm (all other distances remaining unchanged), **XV** is calculated to be 1.36 eV (131 kJ mol^{-1}) less stable than **IV** and to have a higher positive charge on the titanium atom (+0.95 compared with +0.67 in **IV**).

Why then should the phosphine complex $Ti(BH_4)_3(PMe_3)_2$ favour a structure with one BH_4^- ligand co-ordinated in a bidentate manner and the other two each co-ordinated in a 'side-on' fashion along the lines of **XV**? The answer may be found as follows. Consider the interaction of $Ti(BH_4)_3$ in the C_{3h} geometry with regular tridentate BH_4^- ligands (**IV**) with two phosphine ligands oriented along the C_3 axis to generate the structure **XVI**. The phosphine lone pairs give rise to a′

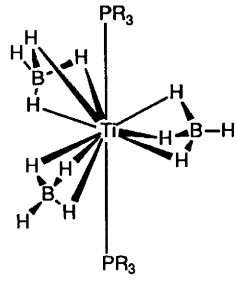

XVI

and a″ symmetry-adapted linear combinations which interact primarily with metal d_{z^2} and p_z orbitals, respectively. The d_{z^2} orbital is therefore strongly destabilised, making it unavailable to accommodate the odd unpaired electron which has to occupy the $Ti(BH_4)_3$ antibonding e″ set derived from d_{xz} and d_{yz} (analogous to 2e″ in Fig. 6). Such a molecule is susceptible to a Jahn–Teller distortion. For a lowering of energy, however, any deformation must destroy the C_3 axis in order to develop the necessary reduction of state degeneracy. Calculations on the model compound $Ti(BH_4)_3(PH_3)_2$ indicate that the observed geometry **I**, approximating to C_{2v} symmetry and with a non-degenerate SOMO, is some 2.9 eV (280 kJ mol^{-1}) more stable than the symmetrical C_{3h} structure represented by **XVI**.

Experimental

Synthesis.—For the synthesis and manipulation of titanium tris(tetrahydroborate) or its fully deuteriated analogue, we found it necessary to work at a pressure $< 10^{-3}$ Torr and under conditions free from any grease or solvent, ideally in Pyrex glass apparatus which had been baked out previously under

Table 6 Nozzle-to-plate distances, weighting functions, correlation parameters, scale factors and electron wavelengths

Molecule	Nozzle-to-plate distance/mm	nm^{-1} Δs	s_{min}	sw_1	sw_2	s_{max}	Correlation, p/h	Scale factor, k[a]	Electron wavelength[b]/pm
$Ti(BH_4)_3$	285.1	2	22	40	125	140	0.3196	0.777(11)	5.963
$Ti(BD_4)_3$	285.2	2	20	40	124	144	0.1469	0.722(9)	5.704
	128.4	4	60	80	250	300	0.0584	0.597(14)	5.704

[a] Figures in parentheses are the estimated standard deviations of the last digits. [b] Determined by reference to the scattering pattern of benzene vapour.

Table 7 Values of parameters utilised in the extended Hückel MO calculations

Atom	Orbital	H_{ii}/eV	ζ_1
Ti	4s	−8.90	1.08
	4p	−6.48	1.08
	3d*	−11.10	4.55
B	2s	−15.20	1.3
	2p	−8.50	1.3
H	1s	−13.60	1.3

*ζ_2 = 1.40, c_1 = 0.4206 and c_2 = 0.7839.

continuous pumping and with distillation pathlengths kept to a minimum. In a typical experiment $TiBr_4$ vapour was drawn slowly through a bed of freshly recrystallised $LiBH_4$ supported on a glass-wool plug and maintained at room temperature. A time of 2–4 d was required for the complete reaction of 2 g (5.4 mmol) of $TiBr_4$ with 1 g (45 mmol) of $LiBH_4$, yielding 0.4 g (4.3 mmol) of $Ti(BH_4)_3$. The volatile products of the reaction were removed under continuous pumping and fractionated between traps held at 255, 195 and 77 K. The $Ti(BH_4)_3$ collected in the 195 K trap. Its purity was assessed by measuring the IR spectrum of the vapour, following systematic studies to determine the effects of contamination by bromotitanium derivatives such as $BrTi(BH_4)_2$ or decomposition products.[20] The synthesis of the perdeuteriated compound, $Ti(BD_4)_3$, followed exactly similar lines. Chemical analysis by methanolysis showed that 1 mol of $Ti(BH_4)_3$ gave typically 12.85 mol of H_2, 3.03 mol of $B(OCH_3)_3$ and 1.065 mol of Ti^{III}, quantities concordant, within experimental error, with equation (2). Samples of the compound were stored in a pre-conditioned glass ampoule at 77 K, until required.

$$Ti(BH_4)_3 + 12CH_3OH \longrightarrow \frac{1}{x}[Ti(OCH_3)_3]_x + 3B(OCH_3)_3 + 12H_2 \quad (2)$$

Spectroscopic Measurements.—Infrared spectra of $Ti(BH_4)_3$ were recorded using either a Perkin-Elmer model 580A dispersive spectrophotometer or a model 1710 FTIR instrument. Matrices were prepared by continuous deposition of $Ti(BH_4)_3$ or $Ti(BD_4)_3$ vapour with an excess of the matrix gas [in the proportions matrix gas:$Ti(BH_4)_3$ or matrix gas:$Ti(BD_4)_3$ = 100:1–500:1] on a CsI window cooled to *ca.* 15 K by means of a Displex refrigerator (Air Products, model CS 202); fuller details of the relevant equipment and procedures for measuring the IR spectra of such matrices are given elsewhere.[46] UV photoelectron spectra of $Ti(BH_4)_3$ vapour were recorded on a Perkin-Elmer PS-16/18 spectrometer, modified for He II measurements by inclusion of a hollow-cathode discharge lamp and high-current power supply (Helectros Developments, Beaconsfield);[8a] calibration made reference to (*i*) He Iα-excited signals due to Xe and Ar and (*ii*) He IIα- and He IIβ-excited helium self-ionisation peaks.

Electron Diffraction Measurements.—Electron-scattering patterns were recorded on Kodak Electron Image plates by using the Edinburgh gas diffraction apparatus.[47] Nozzle-to-plate distances were *ca.* 128 and 285 mm and the accelerating voltage was *ca.* 44 kV (electron wavelength 5.7–6.0 pm). The sample of $Ti(BH_4)_3$ or $Ti(BD_4)_3$ was held at room temperature (*ca.* 290 K) and the vapour gained access to the nozzle of the diffraction apparatus (also at room temperature) *via* a stainless steel needle valve. The plates were usually washed after exposure and left exposed to air for 24 h prior to development in order to minimise the fogging effects of the strongly reducing $Ti(BH_4)_3$ vapour; this is a recurrent problem with hydrido derivatives of the Group 13 elements.[48] The precise nozzle-to-plate distances and electron wavelengths were determined from scattering patterns for benzene vapour recorded immediately before or after the sample patterns. Details are given in Table 6, together with the weighting functions used to set up the off-diagonal weight matrices, the correlation parameters, and final scale factors.

Details of the electron-scattering patterns were collected in digital form by using a computer-controlled Joyce-Loebl MDM6 microdensitometer with a scanning program described elsewhere.[49] Calculations, performed on various computers at the Edinburgh Regional Computing Centre, made use of well established programs for data reduction[49] and least-squares refinement,[50] the complex scattering factors being those listed by Schäfer *et al.*[51]

Extended Hückel MO Calculations.—All the calculations performed utilised the extended Hückel method[17,18] with the weighted H_{ij} formalism.[52] The bond lengths used were as follows: Ti–B (tridentate) 221.8,[16] Ti–B (bidentate) 237,[34a] B–H_b 123 and B–H_t 111 pm. In addition, the analysis drew on the parameters listed in Table 7.[53]

All such calculations were performed on the ICL 2988 computer of the South West Universities Regional Computer Centre by means of the programs ICON8 and FMO.[54]

Acknowledgements

We thank the SERC for the award of research studentships (to C. J. D. and M. J. G.), for financial support of the Edinburgh Electron Diffraction Service, and for provision of the microdensitometer facilities. We are grateful also to Dr. R. G. Egdell who recorded the UV photoelectron spectra of $Ti(BH_4)_3$.

References

1 T. J. Marks and J. R. Kolb, *Chem. Rev.*, 1977, **77**, 263.
2 B. D. James and M. G. H. Wallbridge, *Prog. Inorg. Chem.*, 1970, **11**, 99.
3 J. A. Jensen, J. E. Gozum, D. M. Pollina and G. S. Girolami, *J. Am. Chem. Soc.*, 1988, **110**, 1643; A. L. Wayda, L. F. Schneemeyer and R. L. Opila, *Appl. Phys. Lett.*, 1988, **53**, 361; G. W. Rice and R. L. Woodin, *J. Am. Ceram. Soc.*, 1988, **71**, C181; M. J. Gallagher, W. E. Rhine and H. K. Bowen, *Proceedings of the 3rd International Conference on Ultrastructure Processing of Ceramics, Glasses, and Composites*, eds. J. D. Mackenzie and D. R. Ulrich, Wiley, New York, 1987; R. Bonetti, D. Comte and H. E. Hinterman, *Proceedings of the 5th International Conference on Chemical Vapour Deposition*, Electrochemical Society, Princeton, 1975, p. 495.
4 (*a*) B. D. James, R. K. Nanda and M. G. H. Wallbridge, *Inorg. Chem.*, 1967, **6**, 1979; (*b*) E. E. H. Otto and H. H. Brintzinger, *J. Organomet.*

Chem., 1978, **148**, 29; (*c*) G. E. Toogood and M. G. H. Wallbridge, *Adv. Inorg. Chem. Radiochem.*, 1982, **25**, 267; (*d*) M. L. Luetkens, jun., J. C. Huffman and A. P. Sattelberger, *J. Am. Chem. Soc.*, 1985, **107**, 3361; (*e*) M. D. Fryzuk, S. J. Rettig, A. Westerhaus and H. D. Williams, *Inorg. Chem.*, 1985, **24**, 4316; (*f*) G. G. Hlatky and R. H. Crabtree, *Coord. Chem. Rev.*, 1985, **65**, 1.

5 J. A. Jensen, S. R. Wilson, A. J. Schultz and G. S. Girolami, *J. Am. Chem. Soc.*, 1987, **109**, 8094.

6 A. L. J. Raum and D. A. Fraser, *Br. Pat.*, 801 401, 1958.

7 (*a*) J. C. Bommer and K. W. Morse, *Inorg. Chem.*, 1980, **19**, 587; C. Kutal, P. Grutsch, J. L. Atwood and R. D. Rogers, *Inorg. Chem.*, 1978, **17**, 3558; F. Takusagawa, A. Fumagalli, T. F. Koetzle, S. G. Shore, T. Schmitkons, A. V. Fratini, K. W. Morse, C.-Y. Wei and R. Bau, *J. Am. Chem. Soc.*, 1981, **103**, 5165; (*b*) P. Dapporto, S. Midollini, A. Orlandini and L. Sacconi, *Inorg. Chem.*, 1976, **15**, 2768; C. A. Ghilardi, S. Midollini and A. Orlandini, *Inorg. Chem.*, 1982, **21**, 4096; (*c*) M. V. Baker and L. D. Field, *J. Chem. Soc., Chem. Commun.*, 1984, 996; R. Bau, H. S. H. Yuan, M. V. Baker and L. D. Field, *Inorg. Chim. Acta*, 1986, **114**, L27; (*d*) J. A. Jensen and G. S. Girolami, *J. Am. Chem. Soc.*, 1988, **110**, 4450; *Inorg. Chem.*, 1989, **28**, 2107.

8 (*a*) A. J. Downs, R. G. Egdell, A. F. Orchard and P. D. P. Thomas, *J. Chem. Soc., Dalton Trans.*, 1978, 1755; (*b*) A. P. Hitchcock, N. Hao, N. H. Werstiuk, M. J. McGlinchey and T. Ziegler, *Inorg. Chem.*, 1982, **21**, 793.

9 R. Hoffmann, *Angew. Chem., Int. Ed. Engl.*, 1982, **21**, 711.

10 M. Mancini, P. Bougeard, R. C. Burns, M. Mlekuz, B. G. Sayer, J. I. A. Thompson and M. J. McGlinchey, *Inorg. Chem.*, 1984, **23**, 1072.

11 J. A. Jensen and G. S. Girolami, *J. Chem. Soc., Chem. Commun.*, 1986, 1160; J. A. Jensen, S. R. Wilson and G. S. Girolami, *J. Am. Chem. Soc.*, 1988, **110**, 4977.

12 M. Brookhart and M. L. H. Green, *J. Organomet. Chem.*, 1983, **250**, 395; M. Brookhart, M. L. H. Green and L.-L. Wong, *Prog. Inorg. Chem.*, 1988, **36**, 1.

13 Z. Dawoodi, M. L. H. Green, V. S. B. Mtetwa, K. Prout, A. J. Schultz, J. M. Williams and T. F. Koetzle, *J. Chem. Soc., Dalton Trans.*, 1986, 1629.

14 J.-Y. Saillard and R. Hoffmann, *J. Am. Chem. Soc.*, 1984, **106**, 2006.

15 H. R. Hoekstra and J. J. Katz, *J. Am. Chem. Soc.*, 1949, **71**, 2488; H. Nöth, *Angew. Chem.*, 1961, **73**, 371; B. D. James and M. G. H. Wallbridge, *J. Inorg. Nucl. Chem.*, 1966, **28**, 2456; W. E. Reid, jun., J. M. Bish and A. Brenner, *J. Electrochem. Soc.*, 1957, **104**, 21; K. Franz and H. Nöth, *Z. Anorg. Allg. Chem.*, 1973, **397**, 247; K. Franz, H. Fusstetter and H. Nöth, *Z. Anorg. Allg. Chem.*, 1976, **427**, 97.

16 C. J. Dain, A. J. Downs and D. W. H. Rankin, *Angew. Chem., Int. Ed. Engl.*, 1982, **21**, 534.

17 R. Hoffmann, *J. Chem. Phys.*, 1963, **39**, 1397.

18 R. Hoffmann and W. N. Lipscomb, *J. Chem. Phys.*, 1962, **36**, 2179.

19 (*a*) R. Jungst, D. Sekutowski, J. Davis, M. Luly and G. Stucky, *Inorg. Chem.*, 1977, **16**, 1645; (*b*) F. J. Feher, S. L. Gonzales and J. W. Ziller, *Inorg. Chem.*, 1988, **27**, 3440; (*c*) J. W. Pattiasina, H. J. Heeres, F. van Bolhuis, A. Meetsma, J. H. Teuben and A. L. Spek, *Organometallics*, 1987, **6**, 1004.

20 C. J. Dain, D.Phil. Thesis, University of Oxford, 1981; M. J. Goode, D.Phil. Thesis, University of Oxford, 1987.

21 T. J. Marks, W. J. Kennelly, J. R. Kolb and L. A. Shimp, *Inorg. Chem.*, 1972, **11**, 2540.

22 B. E. Smith, H. F. Shurvell and B. D. James, *J. Chem. Soc., Dalton Trans.*, 1978, 710.

23 T. A. Keiderling, W. T. Wozniak, R. S. Gay, D. Jurkowitz, E. R. Bernstein, S. J. Lippard and T. G. Spiro, *Inorg. Chem.*, 1975, **14**, 576.

24 V. Plato and K. Hedberg, *Inorg. Chem.*, 1971, **10**, 590.

25 R. W. Broach, I-S. Chuang, T. J. Marks and J. M. Williams, *Inorg. Chem.*, 1983, **22**, 1081.

26 R. T. Paine, R. W. Light and M. Nelson, *Spectrochim. Acta, Part A*, 1979, **35**, 213.

27 R. H. Banks, N. M. Edelstein, R. R. Rietz, D. H. Templeton and A. Zalkin, *J. Am. Chem. Soc.*, 1978, **100**, 1957.

28 R. H. Banks and N. Edelstein, *J. Chem. Phys.*, 1980, **73**, 3589.

29 D. A. Coe and J. W. Nibler, *Spectrochim. Acta, Part A*, 1973, **29**, 1789.

30 E. R. Bernstein, T. A. Keiderling, S. J. Lippard and J. J. Mayerle, *J. Am. Chem. Soc.*, 1972, **94**, 2552; E. R. Bernstein, W. C. Hamilton, T. A. Keiderling, S. J. La Placa, S. J. Lippard and J. J. Mayerle, *Inorg. Chem.*, 1972, **11**, 3009.

31 C. J. Dain, A. J. Downs, R. G. Egdell and P. D. P. Thomas, unpublished work; P. D. P. Thomas, D.Phil. Thesis, University of Oxford, 1977.

32 A. Almenningen, G. Gundersen and A. Haaland, *Acta Chem. Scand.*, 1968, **22**, 328.

33 L. S. Bartell and B. L. Carroll, *J. Chem. Phys.*, 1965, **42**, 1135.

34 (*a*) K. M. Melmed, D. Coucouvanis and S. J. Lippard, *Inorg. Chem.*, 1973, **12**, 232; (*b*) G. I. Mamaeva, I. Hargittai and V. P. Spiridonov, *Inorg. Chim. Acta*, 1977, **25**, L123.

35 K. N. Semenenko, E. B. Lobkovskii and A. I. Shumakov, *J. Struct. Chem.*, 1976, **17**, 912.

36 S. J. Lippard and K. M. Melmed, *Inorg. Chem.*, 1967, **6**, 2223; J. T. Gill and S. J. Lippard, *Inorg. Chem.*, 1975, **14**, 751.

37 J. A. Jensen and G. S. Girolami, *Inorg. Chem.*, 1989, **28**, 2114.

38 E. B. Lobkovskii, S. E. Kravchenko and K. N. Semenenko, *J. Struct. Chem.*, 1977, **18**, 312.

39 N. Edelstein, *Inorg. Chem.*, 1981, **20**, 297.

40 See, for example, T. C. De Vore and W. Weltner, jun., *J. Am. Chem. Soc.*, 1977, **99**, 4700.

41 P. G. Eller, D. C. Bradley, M. B. Hursthouse and D. W. Meek, *Coord. Chem. Rev.*, 1977, **24**, 1; D. C. Bradley, *Chem. Br.*, 1975, **11**, 393; J. J. Ellison, P. P. Power and S. C. Shoner, *J. Am. Chem. Soc.*, 1989, **111**, 8044.

42 See, for example, P. Pyykkö and L. L. Lohr, jun., *Inorg. Chem.*, 1981, **20**, 1950.

43 B. M. Gimarc, *Molecular Structure and Bonding*, Academic Press, New York, 1979.

44 R. L. DeKock, K. S. Wong and T. P. Fehlner, *Inorg. Chem.*, 1982, **21**, 3203.

45 J. W. Lauher and R. Hoffmann, *J. Am. Chem. Soc.*, 1976, **98**, 1729.

46 See, for example, M. Hawkins and A. J. Downs, *J. Phys. Chem.*, 1984, **88**, 1527, 3042.

47 C. M. Huntley, G. S. Laurenson and D. W. H. Rankin, *J. Chem. Soc., Dalton Trans.*, 1980, 954.

48 See, for example, M. T. Barlow, C. J. Dain, A. J. Downs, G. S. Laurenson and D. W. H. Rankin, *J. Chem. Soc., Dalton Trans.*, 1982, 597; P. L. Baxter, A. J. Downs, M. J. Goode, D. W. H. Rankin and H. E. Robertson, *J. Chem. Soc., Chem. Commun.*, 1986, 805; M. J. Goode, A. J. Downs, C. R. Pulham, D. W. H. Rankin and H. E. Robertson, *J. Chem. Soc., Chem. Commun.*, 1988, 768; C. R. Pulham, P. T. Brain, A. J. Downs, D. W. H. Rankin and H. E. Robertson, *J. Chem. Soc., Chem. Commun.*, 1990, 177.

49 S. Cradock, J. Koprowski and D. W. H. Rankin, *J. Mol. Struct.*, 1981, **77**, 113.

50 A. S. F. Boyd, G. S. Laurenson and D. W. H. Rankin, *J. Mol. Struct.*, 1981, **71**, 217.

51 L. Schäfer, A. C. Yates and R. A. Bonham, *J. Chem. Phys.*, 1971, **55**, 3055.

52 J. H. Ammeter, H.-B. Bürgi, J. C. Thibeault and R. Hoffmann, *J. Am. Chem. Soc.*, 1978, **100**, 3686.

53 S.-Y. Chu and R. Hoffmann, *J. Phys. Chem.*, 1982, **86**, 1289.

54 J. Howell, A. Rossi, D. Wallace, K. Haraki and R. Hoffmann, *Quantum Chemistry Program Exchange*, 1977, **10**, 344.

Received 17*th August* 1990; *Paper* 0/03791E